ISSN 1936-878X/$36.00
PUBLISHED BY ELSEVIER INC.
DOI:10.1016/j.jcmg.2010.04.013

# In-line Automated Tracking for Ventricular Function With Magnetic Resonance Imaging

Bo Li, MSc,* Yingmin Liu, PhD,* Christopher J. Occleshaw, MBChB,†
Brett R. Cowan, BE MBChB,* Alistair A. Young, PhD*
*Auckland, New Zealand*

An efficient nonrigid registration algorithm was implemented on the image reconstruction computer to enable in-line automatic tracking of features in steady-state free precession cine images. Four-dimensional left ventricle function analysis was performed with and without use of the in-line automatic tracking result. The method was tested in 30 patients referred for cardiac magnetic resonance imaging for a variety of clinical assessments. The time required for in-line tracking was 10 ± 2 s per slice using an image reconstructor with dual Advanced Micro Devices single-core Opteron 248 CPUs (2.2 GHz) and 8GB random access memory. The precision of clinical estimates of left ventricular volumes was significantly improved relative to the ground truth research estimates with automatic tracking versus without (6 ml vs. 9 ml in end-diastolic volume; 5 ml vs. 10 ml in end-systolic volume; both $p < 0.05$). In-line automatic tracking of image features shows promise for facilitating clinical analysis of ventricular function. (J Am Coll Cardiol Img 2010;3:860–6) © 2010 by the American College of Cardiology Foundation

Cardiac magnetic resonance (CMR) imaging is the most accurate and precise method for quantification of left ventricular (LV) mass and volume (1). Calculation of end-diastolic volume (EDV), end-systolic volume (ESV), ejection fraction (EF), stroke volume, and LV mass requires segmentation and tracking of the inner and outer contours of the LV, which is typically performed manually for each contour in a time-consuming and subjective process. Although semiautomated software can assist this process (2), analysis of the many hundreds of images per case represents a significant bottleneck.

Automatic tracking using nonrigid image registration enables tracking of image features from frame to frame by warping images between frames. We have previously shown that off-line automatic tracking using nonrigid registration can provide fast and accurate tracking of endocardial and epicardial contours throughout the cardiac cycle, using a 2-dimensional LV analysis protocol (3).

For these methods to be applied in a clinical environment, an efficient workflow must be achieved by completing the automatic image feature tracking "in-line" on the CMR scanner hardware before display to the operator. Recently, there have been several studies demonstrating the feasibility of in-line processing (4). The purpose of this study was to investigate the feasibility of in-line automatic image feature tracking for the clinical evaluation of LV function. We implemented an efficient automatic nonrigid registration image tracking algorithm on the image reconstruction computer of a standard magnetic resonance imaging scanner. The standard balanced steady-state free precession (SSFP) cine acquisition pulse sequence code was modified to perform in-line auto-

From the *Auckland MRI Research Group, University of Auckland, Auckland, New Zealand; and the †Auckland City Hospital, Department of Cardiology, Auckland, New Zealand. Drs. Cowan and Young have received consulting fees from Siemens AG. This study was funded by the Health Research Council of New Zealand.

Manuscript received March 1, 2010; revised manuscript received April 20, 2010, accepted April 27, 2010.

matic tracking as part of the image reconstruction process. A 4-dimensional (being 3 spatial dimensions plus time) analysis method was adapted to utilize the in-line tracking results in a clinically streamlined analysis protocol designed to maximize throughput while maintaining accuracy and reproducibility. The method was evaluated in 30 patients with cardiovascular disease by comparing results with and without automatic tracking against a research analysis protocol developed for research trial end point evaluation in a core analysis laboratory setting. Figure 1 shows an overview of the 2 analysis pathways compared. We hypothesized that in-line tracking results would facilitate better clinical evaluation of ventricular function.

## Methods

**Automatic image feature tracking.** The image feature tracking algorithm employed was similar to that of Li et al. (3). Briefly, a nonrigid image registration tracking procedure was performed as a warping of a current image to a reference image. The optimal deformation was defined by the minimization of the sum of the squared pixel differences between the reference image and the warped current image.

The parameters of the automatic tracking method were determined by optimizing the match between automatically tracked and manually placed contours in a training set of 36 patients with vascular disease, as described previously (3).

**In-Line Implementation.** The method was implemented on a Siemens (Erlangen, Germany) Avanto 1.5T scanner running the VB15 software version. The image reconstruction computer had dual Advanced Micro Devices (AMD) single-core Opteron 248 processors (2.2. GHz) and 8GB memory. The nonrigid registration algorithm was used to calculate the image warps between consecutive frames of the image sequence, within a 128 × 128 pixel region of interest in the center of the field of view. The Siemens image calculation environment framework was used to implement 3 functors (image calculation environment pipelined computation components), which were inserted into the product image reconstruction functor chain at the end of the reconstruction process. These controlled 1) preparation and dispatch of image registration processes for the multithread implementation; 2) calculation of the image warps between consecutive frames; and 3) collation of results and encoding of the deformation warps into the image headers (Fig. 2). The final deformation maps between each image pair were stored in the DICOM image headers, so that they could subsequently be used for tracking analysis. The image geometric distortion correction option was turned on by default in the acquisition protocol, so that images were corrected for geometric distortions arising from gradient nonlinearities before the registration process.

**Subjects.** Thirty consecutive patients (ages 12 to 75 years, 19 male) were imaged using the modified balanced SSFP pulse sequence, in the course of standard clinical CMR imaging examinations performed at our facility. This study was approved by the institutional review board, and informed consent was obtained. Patients were referred for CMR imaging for a variety of indications, including viability for ischemic heart disease, assessment of cardiomyopathies, and a range of congenital cardiac lesions. Typical imaging parameters were as follows: repetition time, echo time, and flip angle: 27.1 ms, 1.27 ms, and 69°, respectively; parallel acquisition factor 2; segments 9; bandwidth 930 Hz/pixel; field of view 340 × 276.25 mm; image matrix 256 × 208; slice thickness 6 mm; retrospectively gated; 25 cardiac frames reconstructed; and a breath-hold duration of ~12 s. Six equally spaced short-axis slices were acquired spanning the LV from apex to base, together with 3 long-axis slices orthogonal to the short axis and orientated at 60° increments around the central axis of the LV.

**ABBREVIATIONS AND ACRONYMS**

**CMR** = cardiac magnetic resonance
**EDV** = end-diastolic volume
**EF** = ejection fraction
**ESV** = end-systolic volume
**LV** = left ventricular
**SSFP** = steady-state free precession

**Research analysis protocol.** The LV mass and volumes were calculated at each frame in the cine sequence throughout the cardiac cycle using a research analysis protocol, according to the detailed standard operating procedures of our core laboratory, which were developed for the evaluation of research trial end points involving cardiac mass and volume (5). Guide-point modeling (2) was used to adaptively optimize a time-varying 3-dimensional finite element model of the left ventricle to fit each subject's images using custom software (CIM version 6.0). The model was interactively fitted to "guide points" provided by the analyst, as well as computer-generated data points calculated from the image using an edge detection algorithm (Fig. 3), by least-squares

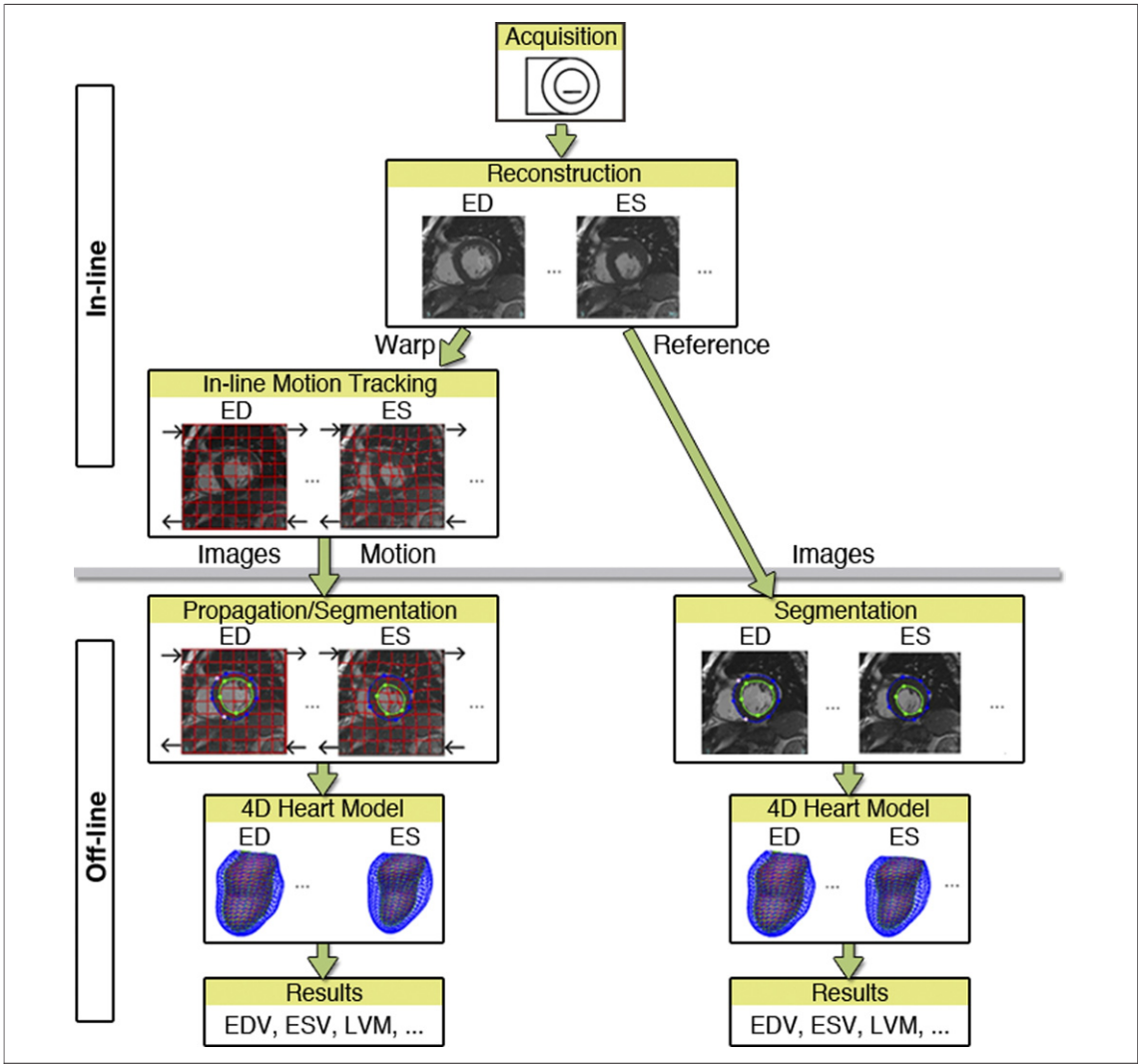


**Figure 1. Overview of the Warp and Reference Analysis Pathways**

ED = end diastolic; EDV = end-diastolic volume; ES = end systolic; ESV = end-systolic volume; 4D = 4-dimensional; LVM = left ventricular mass.

optimization. This method has previously been validated in animals against autopsy LV mass, in patients with regional wall motion abnormalities, against manually drawn contours, and in healthy volunteers against flow-derived measures of cardiac output (2).

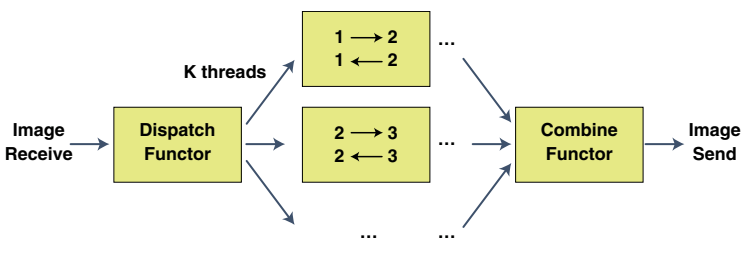


**Figure 2. Schematic of the In-Line Image Registration Process**

Each image was registered with the previous and the next image in the cine sequence, creating forward and backward incremental displacement maps. The computation was shared as equally as possible across all available central processing unit cores (K threads with ~N images per thread). The displacement maps were stored in the image header before export to DICOM format.

**Reference and warp clinical analysis protocols.** The research analysis protocol was modified to maximize throughput in a clinical application setting. This "reference" clinical analysis protocol was performed by a single experienced cardiac radiologist, blinded to the results of other protocols. The analyst concentrated on end-diastolic and end-systolic frames, with fast review of other frames.

The software was modified to take advantage of the image deformation maps calculated by the in-line nonrigid registration procedure, resulting in a "warp" analysis protocol. The warp protocol was the same as the reference protocol, except that contours that were edited were automatically tracked to all other frames using the deformation maps. These "propagated" points were included in the guide point modeling optimization process, with a weighting that decreased linearly with time from the edited frame (Fig. 4). The analyst could correct tracking errors by placing guide points on contours with poorly tracked contours (arising because of through-plane motion or poor contrast to noise ratio). In these cases, the new edited contour was also propagated to surrounding frames in the forward and backward directions.

Mitral valve hinge points were also automatically tracked through each frame using the incremental displacement maps. The analyst could correct tracking errors by manually correcting the mitral valve points, in which case the corrected point was also propagated. The final point for each frame was calculated as a weighted average of the propagated points, with the weights decreasing linearly from the edited frames.

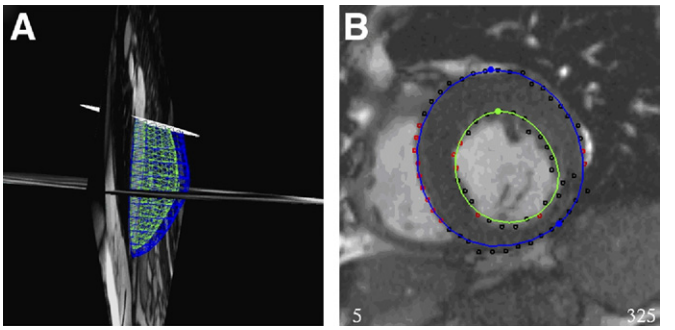


**Figure 3. Three-Dimensional Modeling of Cardiac Function**

**(A)** Three-dimensional display shows left ventricle model with short-axis and long-axis image slices (**green lines** indicate endocardial surface, **blue lines** indicate epicardial surface, **white disk** indicates location of the mitral valve plane). **(B)** Short-axis slice shows user-defined guide points **(green and blue)** and computer-generated image edge points (**black to red**, with color depending on relative edge strength).

The warp analysis was performed by the same clinical analyst, blinded to the results of other protocols (with the study name reanonymized between methods).

**Statistics.** The time taken for 4-dimensional ventricular function assessment using each protocol was compared using a 2-tailed *t* test. Bias (average difference) in EDV, ESV, stroke volume, EF, and LV mass were compared between protocols using a paired 2-tailed *t* test, and Bland-Altman analysis of agreement. The F test was used to compare precision (standard deviation of differences) between protocols. A 0.05 level of significance was chosen.

## Results

The time required for the image reconstruction and registration calculation was 10.1 ± 1.9 s

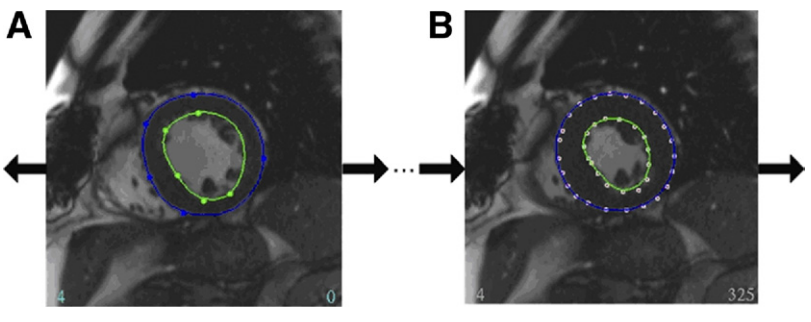


**Figure 4. Propagation of Contour Points Through Time**

**(A)** Short-axis slice showing intersections of the endocardial and epicardial surfaces with the image plane as **green** and **blue** contours, respectively, at end diastole. Dots show location of guide points at end-diastole. **(B)** Locations of contour points propagated from end diastole to end systole **(squares)** using in-line deformation maps.

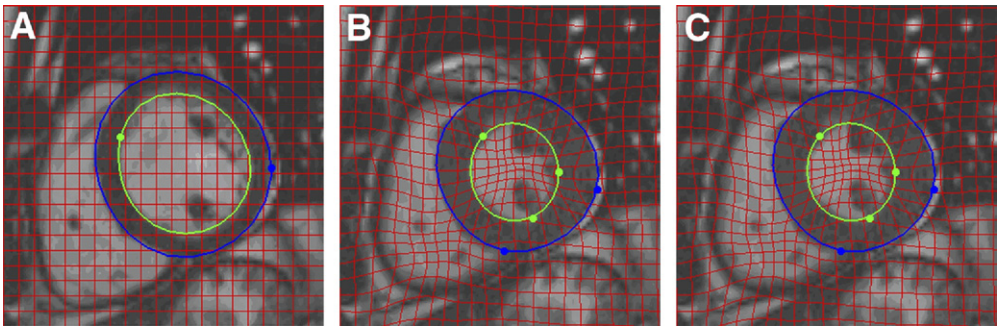


**Figure 5. Deformation Maps**

**(A)** Mid-ventricular short-axis slice at end diastole, with initial rectangular tracking grid **(red)** and manual contours (**green** indicates endocardial, **blue** indicates epicardial; **dots** show location of manually place guide points). **(B)** The same slice at end systole with previously validated off-line tracking (10). **(C)** The same slice at end systole with in-line tracking.

(mean ± SD, range 7.4 to 14.1 s) per slice for a 25-frame acquisition. Of this, <1 s was required for image reconstruction. Deformation maps for the in-line calculation were almost identical with a previously validated off-line calculation (3), as shown in Figure 5.

The time required for the research protocol was 35 ± 10 min (range 17 to 61 min, over both analysts). The time required for the reference clinical protocol was similar to the time required for the warp analysis (8.4 ± 1.7 min vs. 8.3 ± 1.7 min).

Differences in LV volumes and mass between the clinical warp and reference analysis results and the research analysis results are shown in Table 1. The bias (average difference) between LV mass and volumes were small both reference and warp methods. The statistically significant differences in bias in the warp method were not clinically significant, and were due to the high precision (low standard deviations of differences). The precision in EDV and ESV was significantly improved in the warp analysis relative to the reference analysis, with a factor of 2 improvement in ESV. The range of values in this diverse clinical cohort was very large (Table 1) because of the range of ventricular dysfunction encountered in the study patients. Figure 6 shows Bland-Altman plots for differences between each protocol.

## Discussion

Most manufacturers now supply very powerful reconstruction computers that are not heavily used between typical cardiac protocols. This power can be exploited to perform image processing tasks in-line, to facilitate subsequent analysis. The in-line image registration procedure implemented here resulted in an extra delay of ~10 s before images could be displayed to the console. During this delay, scanning can continue. At our institution, we now routinely use the in-line tracking protocol in place of the standard SSFP cine protocol, and queue scans to run when the patient is ready. Given the typical 12-s breath-hold duration and the time required to allow the patient to recover from the breath-hold, this is considered to be feasible clinically.

Over all 30 cases, the warp protocol was not significantly faster than the reference clinical protocol. This may be due to the streamlined clinical protocol performed by the cardiac radiologist who had >10 years experience with the guide point modeling technique. No cases took <5 min because of the time required for model initialization and correction of breath-hold misregistration. However, the precision of the volume estimates were considerably improved in the

**Table 1. Differences in LV Volumes and Mass (Mean ± SD) From Research Results for Reference and Warp Results**

| | EDV (ml) | ESV (ml) | SV (ml) | EF (%) | LV Mass (g) |
|---|---|---|---|---|---|
| Reference | −1 ± 9 | 1 ± 10 | −2 ± 9 | −1 ± 4 | −1 ± 9 |
| Warp | 0 ± 6† | 2* ± 5† | −2 ± 7 | −1* ± 3 | 1 ± 7 |
| Range | 96–436 | 42–314 | 39–166 | 17–69 | 81–251 |

The range for each parameter was calculated from the research results. *$p < 0.05$ for bias between methods. †$p < 0.05$ for precision between methods.
EDV = end-diastolic volume; EF = ejection fraction; ESV = end-systolic volume; LV = left ventricular; SV = stroke volume.

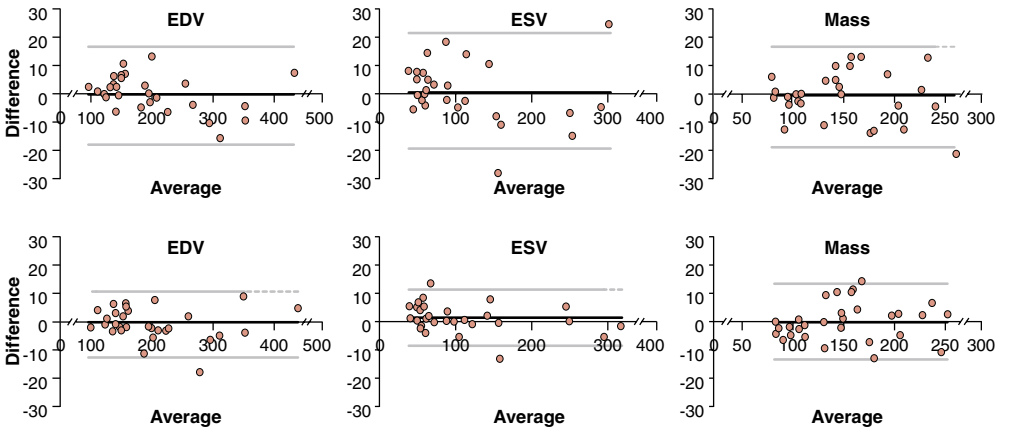


**Figure 6. Bland-Altman Plots of EDV, ESV, and LV Mass Differences**

Bland-Altman plots of end-diastolic volume (EDV), end-systolic volume (ESV), and left ventricular (LV) mass differences from the research protocol, for reference protocol **(top row)** and warp protocol **(bottom row)**. Lines show mean difference ± 2SD.

warp protocol. That improvement may be due to more consistent use of information from all frames in the cine sequence using the automatic in-line tracking results.

The main advantage of the warp method was that the LV mass was automatically constant across the cardiac cycle, which was indicative of consistent automatic feature tracking (Fig. 7). However, mass can be constant despite subtle changes in the placement of the contours. Thus, training is still essential for reproducible LV analysis.

A limitation of the current method was the 128 × 128 region of interest chosen to reduce the computation time to clinically acceptable levels. Although this was found to encompass the heart in all cases, it would be desirable to perform the image warp over the whole field of view. With more processors, or faster computation algorithms, the time required for the automatic tracking is expected to reduce, and the region of interest may be increased, in the future.

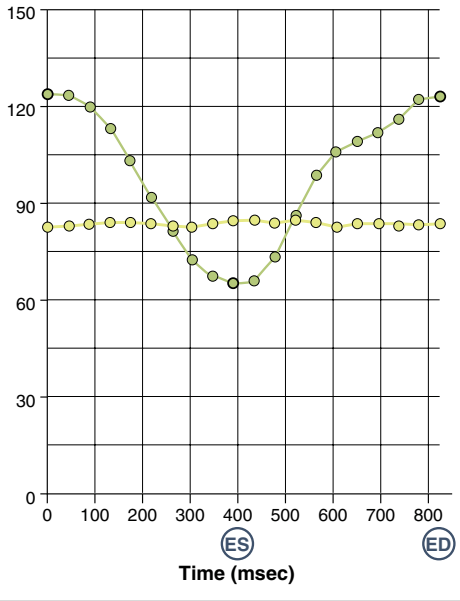


**Figure 7. LV Mass and Volume Across Time**

Left ventricular (LV) mass **(yellow)** and volume **(green)** across time. The LV mass was consistently uniform across the cardiac cycle in the warp method because of image feature tracking. Abbreviations as in Figure 1.

## Conclusions

In conclusion, image feature tracking with nonrigid registration is feasible as part of the image reconstruction process, facilitating faster evaluation of ventricular function. The in-line registration procedure could also be exploited for many other applications, including the estimation of myocardial deformation from tagged images.

### Acknowledgments

The authors would like to thank Jens Guehring, PhD, of Siemens Corporate Research, Princeton, New Jersey, and Andreas Greiser, PhD, of Siemens AG, Erlangen, Germany, for providing helpful comments on the in-line implementation of the registration algorithm.

**Reprint requests and correspondence:** Dr. Alistair A. Young, Department of Anatomy with Radiology, Faculty of Medical and Health Sciences, 85 Park Road, University of Auckland, Auckland 1142, New Zealand. *E-mail: a.young@auckland.ac.nz.*

JACC: CARDIOVASCULAR IMAGING, VOL. 3, NO. 8, 2010
AUGUST 2010:860–6

## REFERENCES

1. Myerson SG, Bellenger NG, Pennell DJ. Assessment of left ventricular mass by cardiovascular magnetic resonance. Hypertension 2002;39:750–5.
2. Young AA, Cowan BR, Thrupp SF, Hedley WJ, Dell'Italia LJ. Left ventricular mass and volume: fast calculation with guide-point modeling on MR images. Radiology 2000;216:597–602.
3. Li B, Young AA, Cowan BR. GPU accelerated non-rigid registration for the evaluation of cardiac function. Med Image Comput Computer Assist Interv 2008;11:880–7.
4. Theisen D, Sandner TA, Bauner K, et al. Unsupervised fully automated inline analysis of global left ventricular function in CINE MR imaging. Invest Radiol 2009;44:463–8.
5. Cowan BR, Young AA, Anderson C, et al. The cardiac MRI substudy to ongoing telmisartan alone and in combination with ramipril global end point trial/telmisartan randomized assessment study in ACE-intolerant subjects with cardiovascular disease: analysis protocol and baseline characteristics. Clin Res Cardiol 2009;98:421–33.

**Key Words:** function ■ nonrigid registration ■ in-line processing.